

Observation of Anisotropy in the Fission Decay of Nuclei with Vanishing Fission Barrier

B. B. Back, H.-G. Clerc,^(a) R. R. Betts, B. G. Glagola, and B. D. Wilkins

Chemistry Division, Argonne National Laboratory, Argonne, Illinois 60439

(Received 23 January 1981)

Fission angular distributions for nuclei formed by fusion of ^{32}S and ^{197}Au , ^{232}Th , ^{238}U , ^{248}Cm show an appreciable anisotropy although spherical saddle-point configurations are predicted for these systems by the rotating-liquid-drop model. The analysis of the data in terms of the statistical model indicate that composite systems of $Z = 106$, 108, and 112 have been formed with deformations $\beta \leq 0.35$.

PACS numbers: 24.75.+i, 25.70.Fg

Several properties of nuclear fission are determined at the fission saddle point, where the energy available for intrinsic excitations is at a minimum.¹ In particular, it is assumed that the final directions of fission fragments are directly related to the orientation of the nuclear symmetry axis during passage over the saddle point. This orientation is expressed in terms of the projections, K and M , of the angular momentum I onto the nuclear symmetry axis and a laboratory fixed axis. At high excitation energies, where the statistical model is applicable, the distribution of K values is expected to be Gaussian² and centered around zero. The variance of this distribution is given by

$$K_0^2 = (T/\hbar^2) \mathcal{G}_{\text{eff}}, \quad 1/\mathcal{G}_{\text{eff}} = 1/\mathcal{G}_{\parallel} - 1/\mathcal{G}_{\perp}, \quad (1)$$

where T is the nuclear temperature at the saddle point and \mathcal{G}_{\parallel} and \mathcal{G}_{\perp} are the moments of inertia associated with rotations around the symmetry axis and a perpendicular axis, respectively. At high temperatures it is expected that the relevant moments of inertia, \mathcal{G}_{\parallel} and \mathcal{G}_{\perp} , approach rigid-body values which then relates the fission angular distribution to the nuclear shape at the saddle point. Analysis of fission-fragment angular distributions obtained in α -particle- and heavy-ion-induced fusion reactions^{3,4} leads to values of \mathcal{G}_{eff} which are in agreement with saddle-point shapes predicted by the liquid-drop model, thereby reinforcing our belief in the correctness of these models of the fission process and nuclear shapes. These data are, however, all associated with nuclei which have well-developed fission barriers at rather large deformations. It is of interest to extend studies of this type to nuclei with vanishingly small fission barriers, such as are expected for nuclei with $Z > 108$ and large angular momenta. In this case, the saddle-point shape is expected to be essentially spherical and should then lead to almost isotropic fission angular distributions. Such studies therefore provide an impor-

tant test of the validity of these theories. Indications of the behavior of such systems have been obtained from the study of sequential fission of heavy products from deep-inelastic reactions.⁵ Values of K_0^2 smaller than those predicted by the liquid-drop model were deduced. The indirect character of the estimation of the charge, mass, excitation energy, spin, and spin alignment of the fissioning nucleus, as well as unknown effects due to the proximity of a third fragment, clearly restricts the accuracy of values of K_0^2 that can be deduced from such measurements. It is therefore more advantageous to study the fission decay of heavy nuclei by producing them in heavy-ion fusion reactions where the parameters describing the compound nucleus can be more precisely specified.

In this Letter we present the measurement of angular distributions for the fission decay of ^{229}Am , $^{264}_{106}\text{X}$, $^{270}_{108}\text{X}$, and $^{280}_{112}\text{X}$ formed in fusion reactions of ^{32}S with ^{197}Au , ^{232}Th , ^{238}U , and ^{248}Cm , respectively. The observed angular anisotropies are substantially larger than those expected on the basis of the rotating-liquid-drop model.⁶

Targets of ^{197}Au , ^{232}Th , ^{238}U , and ^{248}Cm were bombarded with a beam of 218-MeV ^{32}S ions from the Argonne National Laboratory superconducting linac. Fission-fragment angular distributions were measured with the use of a solid-state detector telescope consisting of an 8- μm -thick ΔE detector backed by an E detector of thickness 100 μm . An approximate mass identification of the fission fragments was obtained from the time of flight of the fragments utilizing the time structure of the beam ($\Delta T < 200$ ps). Absolute cross sections for events detected in the telescope were obtained by normalizing to elastic scattering observed in a monitor detector placed at $\theta = 20^\circ$.

In addition, two position-sensitive detectors, placed on opposite sides of the beam at angles of 70° and 80° , were used to measure energies and angles of correlated fission fragments. An analy-

sis of the resulting angular correlation of these fragments indicates that more than 85% of the fission cross section arises from fusion reactions, with the remaining fraction being due to sequential fission of target residues formed in quasielastic or deep-inelastic reactions. Based on this measurement alone, we cannot exclude the possibility that a fraction of the measured cross section arises from incomplete-fusion or massive-transfer reactions. The contribution from these reactions is, however, expected to be negligible at the near-barrier projectile energies used in the present experiment. Centroids of the total-kinetic-energy and mass distributions obtained from the time-of-flight telescope are independent of the scattering angle to within 3%. This observation strongly supports the assumption that the observed fission fragments originate from the decay of an equilibrated composite system and justifies the analysis of the angular distributions within the statistical model.

The angular distributions obtained in the present work are shown in Fig. 1(a). Anisotropies between 2.6 and 5.8 are observed. The solid curves represent the best fits to the data obtained by using the expression

$$W(\theta) = \frac{\sum_{I=0}^{I_{\max}} (2I+1) \sum_{K=-I}^I \frac{1}{2}(2I+1) |\mathfrak{D}_{M=0,K}^I(\theta)|^2 \exp(-K^2/2K_0^2)}{\sum_{K=-I}^I \exp(-K^2/2K_0^2)} \quad (2)$$

which involves summations over I and K of the symmetric-top wave function $\mathfrak{D}_{M=0,K}^I(\theta)$ and assumes a sharp-cutoff expression for the spin distribution and a Gaussian K distribution. The value of I_{\max} used in the analysis was determined from the measured total fission cross sections for which unit fission probability is assumed. The fits to the experimental angular distributions shown in Fig. 1(a) were obtained by varying K_0^2 , which is the only free parameter in this expression. The resulting values of K_0^2 along with the corresponding deduced values of the parameter $\mathcal{g}_0/\mathcal{g}_{\text{eff}}$, where \mathcal{g}_0 is the rigid moment of inertia for spherical shape and \mathcal{g}_{eff} is estimated with use of Eq. (1), are given in Table I.

Theoretical predictions for the fission angular distributions are shown as dashed curves in Fig. 1(a). Saddle-point shapes given by the rotating-liquid-drop model⁶ were used to evaluate the parameters ($\mathcal{g}_0/\mathcal{g}_{\text{eff}}$ and K_0^2) needed to predict the fission angular distributions. We observe that

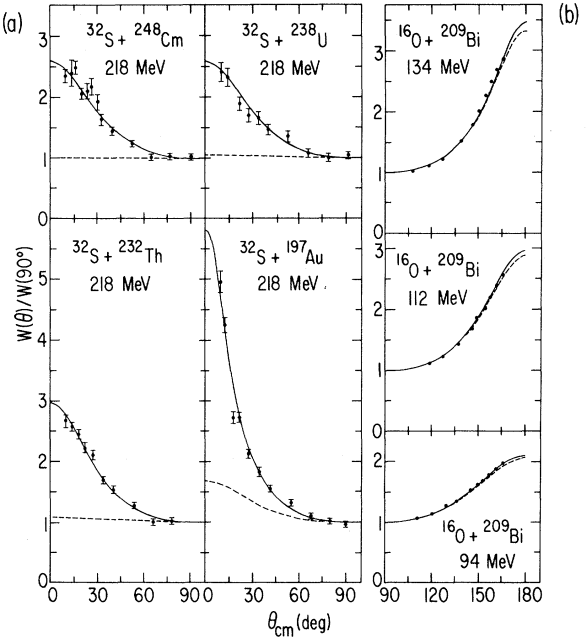


FIG. 1. Experimental fission angular distributions are shown for (a) the four systems studied in the present work; and (b) the reaction $^{16}\text{O} + ^{209}\text{Bi}$, taken from Ref. 5. Full drawn lines represent fits to the data, and dashed curves indicate theoretically expected angular distributions.

the measured anisotropies are severely underestimated by the theory. This discrepancy is taken as a clear indication that the width of the K distribution is not determined at the predicted spherical saddle point, but at a point where the nucleus is more deformed.

The ability of the present model to predict correctly the fission angular distribution for nuclei with a well-developed fission barrier is illustrated in Fig. 1(b), where data for $^{16}\text{O} + ^{209}\text{Bi}$ of Karamyan *et al.*⁴ are described with surprising accuracy by the calculations (dashed curve). It should be noted that in this calculation I_{\max} has been estimated from measured total fission cross sections,⁷ which seems to alleviate the consistency problems observed in earlier analysis of the same data.⁴

Figure 2 further illustrates the correlation between the occurrence of the anomalous angular distributions observed in the present experiment

TABLE I. Parameters used in the angular distribution calculations.

Target	Compound nucleus	x^a	$\langle y \rangle^a$	$W(0^\circ)/W(90^\circ)$	$\sigma_{\text{fis}}^{\text{tot}}$ (mb)	K_0^2	T (MeV)	$\mathcal{J}_0/\mathcal{J}_{\text{eff}}$	β
^{197}Au	^{229}Am	0.817	0.0245	5.18	1110 ± 110	204	1.55	0.89	0.69
^{232}Th	^{264}X	0.899	0.0182	2.96	1080 ± 100	583	1.49	0.38	0.35
^{238}U	^{270}X	0.914	0.0197	2.59	1220 ± 120	840	1.43	0.27	0.25
^{248}Cm	^{280}X	0.948	0.0138	2.59	920 ± 90	640	1.38	0.36	0.33

^aFrom Ref. 7,

$$x = \frac{Z^2/A}{50.883\{1 - 1.7826[(N-Z)/A]^2\}},$$

$$y = \frac{1.9249}{\{1 - 1.7826[(N-Z)/A]^2\}} \frac{I^2}{A^{7/3}}.$$

with the disappearance of the fission barrier for heavy nuclei at high spin. Previous experimental data, for which a detailed analysis of the fission angular distributions have been performed, have, without exception, been obtained for nuclei with a well-developed fission barrier.

We conclude that the present theory for fission angular distributions becomes unreliable as the fission barrier vanishes for heavy, rapidly ro-

tating nuclei. If a statistical equilibrium between intrinsic and rotational degrees of freedom is assumed, it appears that the distribution of K values is not determined at the predicted saddle point, but at a deformation of $\beta \approx 0.25-0.35$, which is between saddle and scission in the cases of $^{32}\text{S} + ^{232}\text{Th}$, $^{32}\text{S} + ^{238}\text{U}$, and $^{32}\text{S} + ^{248}\text{Cm}$. On the other hand, the observation of symmetric fission, which obeys the kinematics for truly sequential processes, indicates a complete equilibration of the composite system prior to fission. It appears that mass and energy equilibrated composite systems of elements $Z=106, 108$, and 112 have been formed with deformations smaller than $\beta \approx 0.35$. The very nature of the statistical-model analysis of the data, however, excludes a determination of the evolution of the K distribution. It is therefore impossible to say if the system has achieved sphericity during its lifetime. In this case, the observed K distribution would result from a suppression of large K values as the system deforms. Alternatively, the width of the K distribution could be a result of a broadening of the initial single-valued $K=0$ distribution by way of exciting tilting and wiggling modes⁹ during the collision.

This work was performed under the auspices of the Office of Basic Energy Sciences, Division of Nuclear Sciences, U. S. Department of Energy.

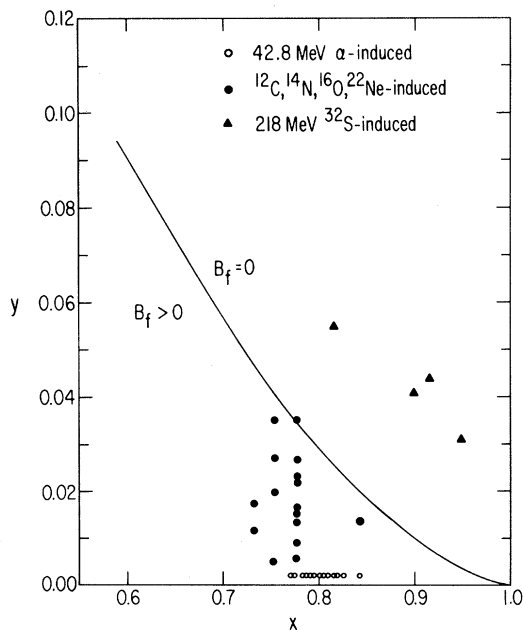


FIG. 2. Maximum angular momenta given by the parameter $y \propto I_{\text{max}}^2$ (see Ref. 7) are compared to the critical value y_{crit} for which the fission barrier vanishes (solid line) as a function of the fissility parameter x . For comparison, the corresponding points for previously studied α -particle- and heavy-ion-induced reactions (from Ref. 8 and Refs. 3 and 4, respectively) are indicated.

^(a)On leave from Institut für Kernphysik, Technische Hochschule Darmstadt, D-6100 Darmstadt, West Germany.

¹Aage Bohr, in *Proceedings of the United Nations International Conference on the Peaceful Uses of Atomic Energy, Geneva, 1955* (United Nations, New York, 1956), Vol. 2, p. 151.

²I. Halpern and V. M. Strutinski, in *Proceedings of*

the *Second United Nations International Conference on the Peaceful Uses of Atomic Energy* (United Nations, Geneva, Switzerland, 1958), p. 408.

³Victor E. Viola, Jr., T. Darrah Thomas, and Glenn T. Seaborg, *Phys. Rev.* **129**, 2710 (1963).

⁴S. A. Karamyan, I. V. Kuznetsov, T. A. Muzycka, Yu. Ts. Oganessian, Yu. E. Penionzkevich, and B. I. Pustyl'nik, *Yad. Fiz.* **6**, 494 (1967) [*Sov. J. Nucl. Phys.* **6**, 360 (1968)].

⁵D. V. Harrach, P. Glässel, Y. Civelekoglu, R. Männer, H. J. Specht, J. B. Wilhelmy, H. Freiesleben, and

K. D. Hildenbrand, in *Proceedings of the Fourth International Atomic Energy Agency Symposium on the Physics and Chemistry of Fission, Jülich, 1979* (International Atomic Energy Agency, Vienna, 1980), Vol. I, p. 575.

⁶S. Cohen, F. Plasil, and W. J. Swiatecki, *Ann. Phys. (N.Y.)* **82**, 557 (1974).

⁷Torbjörn Sikkeland, *Phys. Rev.* **135**, B669 (1964).

⁸R. F. Reising, G. L. Bate, and J. R. Huizenga, *Phys. Rev.* **141**, 1161 (1966).

⁹L. G. Moretto and R. P. Schmitt, *Phys. Rev. C* **21**, 204 (1980).

Determination of the Decay Channel of the $4d \rightarrow 4f$ Resonance in Tm

W. F. Egelhoff, Jr.

Surface Science Division, National Bureau of Standards, Washington, D. C. 20234

and

G. G. Tibbetts

Physics Department, General Motors Research Laboratories, Warren, Michigan 48090

and

M. H. Hecht and I. Lindau

Stanford Synchrotron Radiation Laboratory, Stanford, California 94305

(Received 8 December 1980)

We have found that the shape of the potential for $4f$ electrons in Tm predicts quite well the character of the $4d \rightarrow 4f$ autoionization resonance observed in the photoelectron spectra. The direct photoemission from the $4d$ shell is suppressed by a barrier in the potential. Tunneling through this barrier is significantly slower than the decay of the excited electron back into the $4d$ hole. This decay is thus the dominant channel and is observed to lead predominantly to autoionization of the $4f$ shell.

PACS numbers: 32.80.Dz, 79.60.-i

In several rare-earth solids, pronounced resonances in the photoelectron spectra have been observed in the range of photon energies around the binding energy of the $4d$ shell.¹⁻⁷ They have been interpreted to be due to autoionizing resonances in which the photon excites a $4d$ electron up to the $4f$ shell followed by decay of a $4f$ electron back into the $4d$ hole with the released energy going to ionize a $4f$ electron. These resonances are generally studied with use of constant-initial-state (CIS) spectroscopy in which the electron-energy analyzer is swept in conjunction with the photon energy to record the intensity of photoelectrons originating at a fixed binding energy. Usually the absorption coefficient of the solid is also determined by recording the constant-final-state (CFS) spectrum in which the electron-energy analyzer is fixed at a low kinetic energy to record the intensity of the inelastic secondary electrons as a

function of photon energy. It is generally agreed that the CFS spectrum is directly proportional to the absorption coefficient.⁸ Figure 1 illustrates the parts of the photoelectron spectrum from which the CIS and CFS data are taken. By comparing the two types of spectra we can learn about the relative importance of various excitation and decay channels. The significance of the present work is that for the first time an analysis is made of the influence of the $4f$ potential-energy surface on the character of these resonances, and it is found to be of central importance in understanding such phenomena.

The energy released by the decay of the $4d^9 4f^{n+1}$ intermediate state equals the incident photon energy (unlike in an Auger decay process). The autoionized $4f$ electron thus appears in the photoelectron spectrum as if it had been produced by direct photoionization. Thus at the $4d^{10} 4f^n$